Influence of the postsynthesis preparation procedure on catalytic behaviour of Ag-loaded BEA zeolites in the hydrodechlorination of 1,2-dichloroethane into value added products

A. Śrębowata, R. Baran, G. Slowik, D. Lisovytskiy, Stanislaw Dzwigaj

Influence of the postsynthesis preparation procedure on catalytic behavior of Ag-loaded BEA zeolites in the hydrodechlorination of 1,2-dichloroethane into value added products

A. Śrębowata[1,*], R. Baran[2,3,4], G. Słowik[5], D. Lisovytskiy[1], S. Dzwigaj[3,4,*]

[1]Institute of Physical Chemistry, PAS, Kasprzaka 44/52, PL-01224 Warszawa, Poland,

[2]AGH University of Science and Technology al. A. Mickiewicza 30, 30-059 Krakow, Poland

[3]Sorbonne Universités, UPMC Univ Paris 06, UMR 7197, Laboratoire de Réactivité de Surface, F-75005, Paris, France

[4]CNRS, UMR 7197, Laboratoire de Réactivité de Surface, F-75005, Paris, France

[5]Faculty of Chemistry, Department of Chemical Technology, Maria Curie – Skłodowska University, Plac Marii Curie – Skłodowskiej 3, PL-20-031 Lublin, Poland

***Corresponding authors**

Anna Srebowata, E-mail: asrebowata@ichf.edu.pl, Tel. 48 1 22 343 3320

Dzwigaj Stanislaw, E-mail : stanislaw.dzwigaj@upmc.fr, Fax : 33 1 44 27 21 13

Graphical Abstract

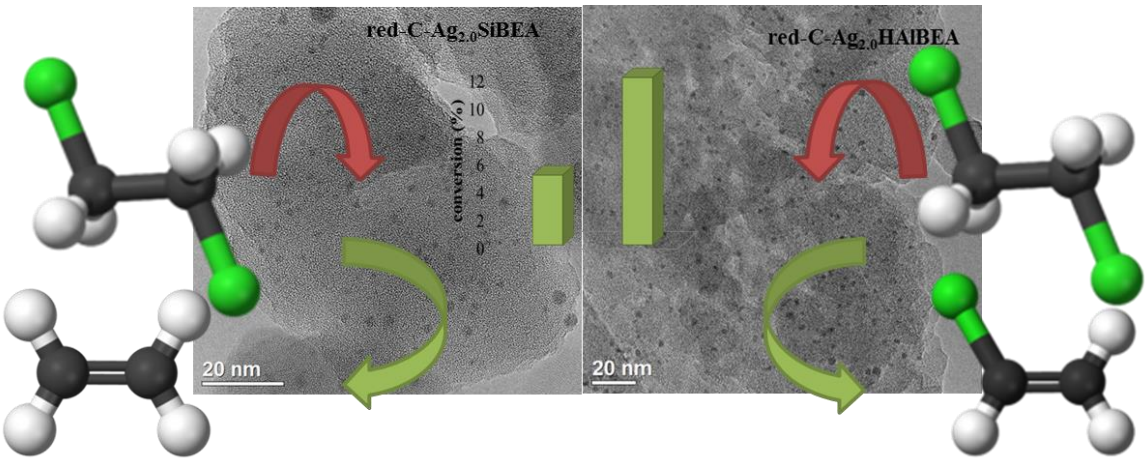

Highlights

- Unique activity of Ag-loaded BEA zeolites in hydrodechlorination of 1,2-dichloroethane
- Red-C-$Ag_{2.0}$SiBEA showed ~ 100 % selectivity to ethylene
- Activity of red-C-$Ag_{2.0}$HAlBEA depended on their acidity
- Red-C-$Ag_{2.0}$HAlBEA promoted formation of ~ 100 % of vinyl chloride
- Only large Ag nanoparticles transform into AgCl upon HDC reaction

Abstract

Two silver-containing BEA zeolites prepared by a two-step postsynthesis method ($Ag_{2.0}$SiBEA) and a conventional wet impregnation ($Ag_{2.0}$HAlBEA) showed a high activity in the conversion of 1,2-dichloroethane (1,2-DCE) into value added products with 100% selectivity into ethylene and 100 % selectivity into vinyl chloride, respectively. The role of the silver in two kinds of studied catalysts was different. The HRTEM, STEM with EDS elemental mapping showed that the excellent activity of silver containing catalyst, prepared by two-step postsynthesis method, in hydrodechlorination of 1,2-DCE was strongly related to the presence of very small (< 3 nm) metallic nanoparticles, resistant for the deactivation by chlorine poisoning. On the other hand, introduction of Ag ions into the HAlBEA zeolite led to

a decrease of the coke formation during hydrodechlorination process on red-C-$Ag_{2.0}$HAlBEA zeolite catalyst. As a result, it was observed lower drop of activity of red-C-$Ag_{2.0}$HAlBEA catalyst than HAlBEA over HDC reaction ~~was observed~~ with maintaining 100% selectivity to vinyl chloride.

Keywords: Ag, zeolite, 1,2-dichloroethane, hydrodechlorination, value added products

1. Introduction

One of the most important environmental problems is contamination of the atmosphere, the soil and the ground water by chlorine containing volatile organic compounds (Cl-VOCs). Due to the high volatility and resistance to degradation they pose a serious threat to the human health and life. Therefore, there is needed a new technology that would efficiently remove these harmful, usually mutagenic and carcinogenic chemicals from environment [1].

An attractive, environmentally friendly method of "utilization" of Cl-VOC's is hydrodechlorination (HDC). The interest in this method has increased since the early nineties of 20^{th} century. [2]. In the contrast to the combustion of Cl-VOCs [3,4], catalytic oxidation [5], plasma destruction [6], pyrolysis [7] and HDC lead to the formation of useful and/or environmentaly friendly products. It was reported that the efficient catalysts in hydrodechlorination are noble metals such as palladium and platinum [8-12] and noble metals doped with Co, Cu, Ni, Fe or Ag [13-20]. Notwithstanding, as an alternative to expensive precious-metals-supported catalysts, it has been proposed to use containing catalysts, which also lead to high selectivity to value added products [21-24]. Depending on the kind of the support, application of nickel containing materials lead~~s~~ to the formation of unsaturated hydrocarbons and/or less chlorinated hydrocarbons, such as ethylene and vinyl chloride in the case of HDC of 1,2-dichloroethane [20,21].

Ag-supported catalysts have been extensively used in NO_x abatement [25], the selective catalytic reduction of NO [26], the selective catalytic oxidation of ammonia [27], CO

oxidation [28] or ethylene epoxidation [29] as well as in hydrogenation of C=O groups in the presence of a C=C bond [30]. Moreover, silver plays also very important role in bimetallic catalytic systems [31,32]. For example, the bimetallic catalyst based on palladium with addition of silver was applied for selective hydrodechlorination of 1,2-dichloroethane [32].

Our thorough analysis of the literature data did not unearth any studies of catalytic activity of monometallic silver catalysts in 1,2-dichloroethane hydrodechlorination. However, our recent work on the activity of zeolite containing bimetallic Ni-Ag systems showed unexpected activity of monometallic silver-containing BEA zeolite catalyst in HDC reaction [33]. We postulated that this unique activity of Ag is related to the presence of very small Ag(0) nanoparticles. Therefore, the aim of this study is the detailed examination of the ~~causes~~ reasons of the high activity of red-C-AgSiBEA catalyst and the investigation of the influences of the preparation procedures on the properties of Ag-containing BEA zeolite catalysts in the selective conversion of 1,2-dichloroethane into value added products.

Red-C-$Ag_{2.0}$HAlBEA and red-C-$Ag_{2.0}$SiBEA zeolites prepared by conventional wet impregnation and two-step postsynthesis procedure, respectively, were characterized by UV-Vis spectroscopy (DR UV-Vis), temperature-programmed reduction (TPR) and X-ray diffraction (XRD). To determine the nanoparticles size distribution in reduced and spent-catalysts HRTEM, STEM with elemental mapping and phase identification were used.

2. Experimental

2.1 Catalysts synthesis

A tetraethylammonium BEA (TEABEA) (Si/Al = 17, with 2.7 wt % of Al and 44.2 wt % of Si) zeolite provided by RIPP (China) was calcined in air (100 K h^{-1}) at 823 K for 15 h under static condition to remove the organic template. Organic-free BEA zeolite was separated into two portions. The first portion was treated with 13 mol· L^{-1} nitric acid solution

(353 K, 4 h) to obtain dealuminated SiBEA zeolite (Si/Al = 1500, with 0.02 wt % of Al and 46.6 wt % of Si) and then washed several times with distilled water and dried at 363 K overnight. Second fraction of calcined BEA zeolite was treated two times with 0.1 mol L^{-1} NH_4NO_3 solution during 3 h in order to exchange K^+ and Na^+ ions present in industrial BEA zeolite, for NH_4^+ ion. Then, the solid was washed with distilled water and dried overnight at 363 K. The NH_4AlBEA sample was calcined in air (100 K· h^{-1}) for 3 h at 773 K under static condition to remove NH_3 and obtain acidic form of zeolite BEA, HAlBEA (Si/Al = 20, with 2.2 wt % of Al and 44.2 wt % of Si).

In order to obtain $Ag_{2.0}$HAlBEA and $Ag_{2.0}$SiBEA zeolites, 2 g of HAlBEA or SiBEA were impregnated with aqueous solutions of $AgNO_3$, respectively. In an initial stage of the preparation process the suspensions were stirred for 24 h at ambient temperature in excess solvent. In the following step, samples were stirred in evaporator under vacuum of a water pump for 2 h in air at 333 K until water removal.

After that, as prepared $Ag_{2.0}$HAlBEA and $Ag_{2.0}$SiBEA were calcined at 773 K for 3 h in air flow (50 mL · min^{-1}) and labelled as C-$Ag_{2.0}$HAlBEA (Si/Al = 20, with 2.2 wt % of Al and 44 wt % of Si, and 2.0 wt % of Ag) and C-$Ag_{2.0}$SiBEA (Si/Al =1500, with 0.02 wt % of Al and 46.4 wt % of Si, and 2.0 wt % of Ag), respectively (where C stand for calcined). Finally, C-$Ag_{2.0}$HAlBEA and C-$Ag_{2.0}$SiBEA materials were reduced at 873 K, for 3 h in flowing 10 % H_2/Ar to obtain red-C-$Ag_{2.0}$HAlBEA and red-C-$Ag_{2.0}$SiBEA, respectively (where red stand for reduced).

2.2. Characterization techniques

DR UV–vis spectra of as prepared, calcined and reduced samples were recorded at ambient atmosphere on a Cary 5000 Varian spectrometer equipped with a double integrator with polytetrafluoroethylene as reference.

Temperature-programmed reduction (TPR) was carried out using the glass-flow system. TPR runs were conducted in flowing 10 % H_2/Ar (25 mL· min^{-1}), ramping the temperature from ambient to 1123 K with step of 10 K· min^{-1} and using a Gow-Mac thermal conductivity detector (TCD). Injections of known amounts of hydrogen into the hydrogen–argon flow were provided for calibration (before and after each TPR run).

X-ray driffractograms (XRD) were recorded in ambient atmosphere on Geigerflex Rigaku-Denki (Japan) diffractometer with nickel filtered and CuK_α radiation. Data acquisition for sample after reduction step and after kinetic run were recorded in the 2 θ range of 5 - 90º with step of 0.02º.

HRTEM studies were carried out for containing silver zeolites after reduction and after catalytic tests. The catalysts were grinded in an agate mortar to a fine powder. The resulting powder was suspended in 99.8% ethanol (POCH) to form a slurry. The sample was inserted into the ultrasonic homogenizer for 20 s. Then, the slurry containing the catalyst was pipetted and supported on a 200 mesh copper grid and stabilized with carbon (Ted Pella Company) and left on the filter paper until the ethanol has evaporated. Subsequently, the sample deposited on the grid was inserted to holder and moved to electron microscope. The electron microscope Titan G2 60-300 kV FEI Company, equipped with: field emission gun (FEG), monochromator, three condenser lenses system, the objective lens system, image correction (Cs-corrector), HAADF detector and EDS spectrometer (Energy Dispersive X -Ray Spectroscopy) EDAX Company with detector Si(Li) was used to display the prepared catalysts. Microscopic studies of the catalysts were carried out at an accelerating voltage of the electron beam equal to 300 kV.

2.3. Catalysts activity

The hydrodechlorination reaction (HDC) of 1,2-dichloroethane (1,2-DCE, pure 99,8% from Sigma-Aldrich, Germany) was carried out with two series of zeolite catalysts: red-C-

$Ag_{2.0}$HAlBEA and red-C-$Ag_{2.0}$SiBEA. Prior to reaction, 0.2 g of C-$Ag_{2.0}$HAlBEA and C-$Ag_{2.0}$SiBEA zeolites were reduced in flowing 10 % H_2/Ar (25 mL· min^{-1}), ramping the temperature from 298 to 873 K (at 10 K· min^{-1}) and kept at 873 K for 3 h. Subsequently, the catalysts were cooled down into 523 K and contacted with the reaction mixture (H_2 + Ar + 1,2-DCE). Total gas flow was 42 mL · min^{-1}. 1,2-DCE was provided from a saturator kept at 273 K. The partial pressure ratio p(H_2)/p(1,2-DCE) was 1:1. The flows of H_2 and Ar were fixed by using Bronkhorst Hi-Tec mass flow controllers. The contact time was τ = 0.7 s and the space velocity was SV= 0.0035 ($m^3 \cdot kg^{-1} \cdot s^{-1}$). The exhaust gas stream was analyzed with gas chromatography, using a HP 5890 series II Hewlett Packard (USA), gas chromatograph with FID detector, a 5 % Fluorcol/Carbopac B Supelco (USA) column (10 ft). The results of GC analysis were elaborated using HP Chemstation.

3. Results and discussion

The state of silver in Ag-containing BEA zeolites was investigated by DR UV-vis and H_2-TPR

3.1. Diffuse reflectance UV–vis investigation

In general, as reported earlier for Ag/zeolite A [34,35] the electronic structure of a silver-containing zeolite material can be seen as a superposition of the electronic structure of the framework and the silver species. According to earlier studies [36,37] depending on the state of silver, DR UV-vis adsorption bands appear at wavelength of 210 - 500 nm. The absorbance in the region below 250 nm is generally attributed to electronic transitions from $4d^{10}$ to $4d^9 5s^1$ of highly dispersed Ag^+ ions. The absorption bands in the range of 250 - 390 nm are commonly ascribed to silver clusters ($Ag_n^{\delta+}$ with $n \leq 8$) with a variety of cluster sizes and/or different oxidation states. The absorption at wavelengths > 370 nm is attributed to nanoparticles of metallic silver [38].

As it is showed in **Figure 1** and **2,** in DR UV-vis spectra of as prepared $Ag_{2.0}$HAlBEA and $Ag_{2.0}$SiBEA two bands at 214 and 270-305 nm are present related to the charge transfer transition between $4d^{10}$ and $4d^{9}5s^{1}$ level of highly dispersed Ag^{+} species and charge transfer transitions in BEA framework, respectively, in line with earlier reports for Ag-MFI zeolites, Ag/Al_2O_3, Ag^{+}/ZSM-5 and AgBEA [36,39-42]. The absence of the bands at higher wavelength between 350 and 500 nm suggests that silver nanoclusters ($Ag_n^{\delta+}$) and metallic silver nanoparticles are not present in as prepared $Ag_{2.0}$HAlBEA and $Ag_{2.0}$SiBEA.

The disappearance of the band at 214 nm and appearance of new bands in the range of 260 -520 nm, at 286, 309, 405 and 520 nm for C-$Ag_{2.0}$HAlBEA and at 266 and 420 nm for C-$Ag_{2.0}$SiBEA (**Figures 1 and 2**) may suggest the formation of $Ag^{n\delta+}$ clusters and silver nanoparticles with different average size diameter under calcination condition [38,43].

Further treatment of C-$Ag_{2.0}$HAlBEA and C-$Ag_{2.0}$SiBEA with flowing 10 % H_2/Ar leads to decrease of the intensity of the bands in the range of 260 - 420 nm (**Figures 1** and **2**) due to the reduction of silver oxide nanoclusters ($Ag_n^{\delta+}$) and formation of Ag^0 nanoparticles. New bands appeared at 209, 223, 426 and 520 nm for red-C-$Ag_{2.0}$HAlBEA and at 209, 223 and 405 nm for red-C-$Ag_{2.0}$SiBEA are probably related to existence of highly dispersed Ag^{+} ions (209 nm) [38] and the formation of Ag^0 nanoparticles, in line with earlier report on Ag-containing materials [37,39].

3.2. Temperature – programmed reduction results

Temperature-programmed reduction experiments were carried out to determine the reducibility of silver in C-$Ag_{2.0}$HAlBEA and C-$Ag_{2.0}$SiBEA zeolites. For both zeolite samples low intense reduction peaks at temperature 313 and 366 K for C-$Ag_{2.0}$HAlBEA and at 312 for

C-$Ag_{2.0}$SiBEA are observed, respectively, in **Figure 3**. These low temperature reduction peaks could be assigned to the reduction of well dispersed mononuclear Ag(I) and/or silver oxides to metallic Ag^0 form, in agreement with earlier works on silver based catalysts [26,44].

Additionally, TPR pattern of C-$Ag_{2.0}$HAlBEA contains two main peaks at 466 and 624 K as well as small one at 765 K. The observed peaks may be attributed to the reduction of silver present in three different states. The first of them can be attributed to the reduction of Ag_2O present in extra-framework positions. Two reduction peaks with the maximum at higher temperature may be assigned to reduction of silver species (Ag^+ ions) at exchange positions and/or strongly interacting with zeolite support (probably two types of silver species) [45].

On the other hand, TPR pattern of C-$Ag_{2.0}$SiBEA in **Figure 3**, except low temperature peak, contains two peaks at 645 and 744 K. Similarly, like in the case of the results obtained for C-$Ag_{2.0}$HAlBEA, they could be attributed to reduction of excellent dispersed silver species most probably present as mononuclear isolated Ag(I). The difference between the position of the peak maximum on TPR patterns for C-$Ag_{2.0}$HAlBEA and C-$Ag_{2.0}$SiBEA could be related to the synthesis procedure. For C-$Ag_{2.0}$SiBEA, some part of silver could strongly interact with zeolite support and is more resistant for reduction process.

Although both of Ag-containing zeolites comprise the same Ag content, TPR pattern of C-$Ag_{2.0}$SiBEA shows lower hydrogen consumption than C-$Ag_{2.0}$HAlBEA. Thanks to injections of known amounts of hydrogen into the hydrogen–argon flow before and after each TPR run, the quantitative estimation of the amount of reduced Ag in the both samples were possible. Calculations obtained for C-$Ag_{2.0}$SiBEA showed degree of reduction of 78%. On the other hand, the degree of reduction of 100% was achieved for C-$Ag_{2.0}$HAlBEA. According to Popovych et al. [26], this phenomenon may be caused by the problem of reduction of Ag incorporated into the framework position of SiBEA and/or the formation of metallic silver nanoparticles during calcination process.

3.3. Catalytic activity of red-C-Ag$_{2.0}$HAlBEA and red-C-Ag$_{2.0}$SiBEA

In the **Figure 4** are showed the differences of the 1,2-dichloroethane conversion in hydrodechlorination of 1,2-DCE between all studied catalysts**.** The catalytic activities of red-C-HAlBEA support and red-C-Ag$_{2.0}$HAlBEA zeolite catalyst are very similar, in particular during the first hours of the reaction. It suggests that the Ag(0) nanoparticles present in red-C-Ag$_{2.0}$HAlBEA zeolite catalyst did not significant influence ~~on~~ the catalytic properties of this catalyst in hydrodechlorination of 1,2-dichloroethane. The very high (~ 100%) selectivity towards vinyl chloride for both zeolite catalysts indicates (**Fig. 5**) that transformation of 1,2-dichloroethane into vinyl chloride ~~to~~ goes on Brønsted acidic sites numerously present in both zeolites in line with our report on Ni-containing HAlBEA zeolite catalyst and HAlBEA support [21]. On the other hand, it should be noticed here that the activity of red-C-Ag$_{2.0}$HAlBEA decreased slower in time than it was observed for red-C-HAlBEA (**Fig. 4**). This phenomenon is probably related to decrease in the amount of strong Brønsted acidic sites due to partial ion exchange between proton of bridging hydroxyls Si-O(H)-Al groups with silver ions upon introduction of Ag into the HAlBEA zeolite. Similar observations were already reported in our previous work [42]. Such a zeolite modification resulted in a decrease of the cock formation upon hydrodechlorination process on red-C-Ag$_{2.0}$HAlBEA and in the consequence a lower drop of 1,2-dichloroethane conversion.

As it is seen in **Figure 4,** the activity of dealuminated form of BEA zeolite (red-C-SiBEA support) in HDC is negligible with 1,2-dichloroethane conversion of 0.5 %. In contrast, red-C-Ag$_{2.0}$SiBEA zeolite catalyst shows significant activity in HDC with 1,2-dichloroethane conversion of about 4 % and very high selectivity towards ethylene (100 % during several hours of reaction test (**Fig. 6**.)). Additionally, red-C-Ag$_{2.0}$SiBEA zeolite catalyst is very stable in hydrodechlorination of 1,2-dichloroethane (**Fig. 4**) as shown by the

similar 1,2-dichloroethane conversion during 17 h of the reaction without signs of deactivation.

In the Figures 5 and 6 the results of selectivity to vinyl chloride and ethylene are showed respectively. Due to the presence of traces of strong Brønsted acidic sites, the main product obtained for red-C-SiBEA was vinyl chloride (**Fig. 5**) and selectivity towards ethylene was almost zero due to the absence of silver. On the other hand, for red-C-$Ag_{2.0}$SiBEA containing well dispersed small Ag(0) nanoparticles, 100% selectivity towards ethylene was achieved. Furthermore, the durability experiment with red-C-$Ag_{2.0}$SiBEA showed very high stability of this catalysts and constant selectivity to ethylene during ~67 h of 1,2-dichloroethane hydrodechlorination (**Fig. 7)**.

The comprehensive review of the literature did not unearth any experimental study of HDC of 1,2-dichloroethane on monometallic silver supported on BEA zeolite. Therefore it is very difficult to compare our results with other works. Presence of silver usually influences catalytic behaviour of noble metals such as Pd and Pt in hydrodechlorination [16,17,49]. Normally, an addition of Ag to noble metal (Pd or Pt) containing catalysts improves ethylene selectivity during HDC of 1,2-dichloroethane, as reported earlier [16,17,49]. Pirard et al. [49] determined the role of silver in the formation of ethylene on ~~over~~ bimetallic Pd-Ag/SiO_2 catalyst. By the using an experimental setup design with five independent variables~~:~~ (temperature and partial pressures of 1,2-dichloroethane, hydrogen, ethylene and hydrogen chloride) they revealed that hydrodechlorination of 1,2-dichloroethane on Pd-Ag/SiO_2 correspond to a Langmuir–Hinshelwood model involving two types of active sites and the 1,2-dichloroethane adsorption as rate-determining step. Moreover, they reported that HDC of 1,2-dichloroethane into ethylene occurs on silver sites through dissociative adsorption with successive brakeage of the two C–Cl bonds and desorption of ethylene. However, it was postulated that silver necessarily “needs” the source of atomic form of hydrogen, otherwise is

deactivated by adsorbed chlorine anions [16,17,20,49]. In the case of bimetallic palladium – silver system this role has been played by Pd, which thanks to its activation power of hydrogen by dissociative chemisorption, supplies hydrogen atoms for the regeneration of the chlorinated silver surface into metallic silver. Thus, the occurrence of Ag and noble metal alloys is crucial in order to obtain active catalyst with very high selectivity toward desired products [16,17,49]. The lack of such a system led to the irreversible deactivation of silver sites by chlorine poisoning. Therefore, very good catalytic behaviour of red-C-$Ag_{2.0}$SiBEA may be related to the presence of poison-resistant silver nanoparticles. So it is extremely interesting to find the reason of this unique activity.

It is well known that the catalytic behaviour of different materials in HDC reaction is strongly dependent on metal(s) particles size. Generally, smaller metal particle sizes, and thereby, higher metal surface areas could favourably impact on catalytic activity, selectivity and stability of metal(s)/support systems in HDC [21,50,51]. Due to the very low activity of monometallic silver catalysts in 1,2-dichloroethane hydrodechlorination, authors did not concentrate on determination of the silver particles size [16,17]. However, Pirard et al. [49] postulated that catalytic behaviour of silver containing catalysts in HDC of 1,2-dichloroethane should be attributed to the presence of Ag(0) nanoparticles with small size. It was indirectly confirmed by Lambert et al. [18] who postulated that the large silver nanoparticles are inactive in hydrodechlorination of 1,2-dichloroethane. Therefore, according to Pirard et al. [49] and Lambert et al. [18] good catalytic behaviour of red-C-$Ag_{2.0}$SiBEA in HDC of 1,2-dichloroethane should be attributed to the presence of Ag(0) nanoparticles with small size. Babu et al. [50] suggested that the presence of smaller Ag nanoparticles promotes electron transfer from metal to the support. Thus, the cationic $Ag_n^{\delta+}$ clusters are more resistant to deactivation by chlorine adsorption and red-C-$Ag_{2.0}$SiBEA zeolite catalyst remains active during the reaction. The catalytic behaviour of red-C-$Ag_{2.0}$SiBEA is very similar to the one of

Au/Fe_2O_3 with excellent dispersed gold nanoparticles of average size 2.6 nm [52]. Although overall conversion obtained for red-C-$Ag_{2.0}$SiBEA was slightly smaller or comparable to that obtained for other materials in hydrodechlorination of 1,2-dichloroethane (**Figs. 4,7**) [8-24], it should be noted that this is the first report where significant activity of monometallic silver nanoparticles formed in zeolite catalyst in HDC process was achieved.

The results of physicochemical characterization and catalytic tests suggest that the active species of 1,2-dichloroethane hydrodechlorination towards ethylene are small and well dispersed silver(0) nanoparticles. On the other hand, transformation of 1,2-dichloroethane into vinyl chloride takes place on Bronsted acidic centers present in red-C-HAlBEA and red-C-$Ag_{2.0}$HAlBEA. The detailed information of the reaction mechanism was published in our earlier work [21]. The formation of well dispersed Ag(0) species in red-C-$Ag_{2.0}$SiBEA was possible due to the application of the two-step postsynthesis method for catalysts preparation. The isolated Ag(I) species occurring in the framework positions of C-$Ag_{2.0}$SiBEA were transformed during H_2 treatment into small silver(0) nanoparticles.

3.4. HRTEM and STEM investigation

The insightful HRTEM, STEM and EDS elemental mapping was carried out to identify silver particles size and to help clarify the cause of unique activity of silver containing zeolites in HDC reaction.

Figures 8 and **9** exhibit HRTEM images and histograms of silver nanoparticles size distribution for red-C-$Ag_{2.0}$HAlBEA, spent-red-C-$Ag_{2.0}$HAlBEA, red-C-$Ag_{2.0}$SiBEA and spent-red-C-$Ag_{2.0}$SiBEA.

For red-C-$Ag_{2.0}$HAlBEA the silver nanoparticles are well dispersed in the zeolite structure and an average silver particle size is ~ 4 nm. The silver nanoparticles with the size of 2-6 nm formed in red-C-$Ag_{2.0}$HAlBEA might be due to incorporation of part of Ag^+ ions in

vacant-T-atoms sites of parent HAlBEA support, in line with our earlier work [21]. The results obtained for spent-red-C-$Ag_{2.0}$HAlBEA catalysts (**Fig. 8**) show the particles larger (average particles size of 5.5 nm) than that observed for the catalysts after reduction step.

In red-C-$Ag_{2.0}$SiBEA silver nanoparticles are well dispersed with the average metal particles size of 3.2 nm (**Fig. 9**). Besides of this very small silver nanoparticles, larger Ag(0) nanoparticles were also observed (**Fig. 9**). The similar distribution of Ag(0) nanoparticles was evidenced for spent-red-C-$Ag_{2.0}$SiBEA (**Fig. 9**). It suggests that sintering of Ag(0) nanoparticles during hydrodechlorination of 1,2-dichloroethane practically did not occur. It seems that this is the reason of high stability of red-C-$Ag_{2.0}$SiBEA during HDC process, as shown in **Figures 4 and 7** in chapter 3.3.

HRTEM comparison studies for C-$Ag_{2.0}$HAlBEA and C-$Ag_{2.0}$SiBEA after reduction at 873 K and after catalytic run suggest a lower sintering resistance of silver present in red-C-$Ag_{2.0}$HAlBEA zeolite catalyst. In contrast, red-C-$Ag_{2.0}$SiBEA contains mainly very small silver nanoparticles which are resistant to sintering.

Authors of the earlier works [18,49] devoted to HDC on silver containing catalysts, postulate, that the lack of activity of monometallic silver samples in hydrodechlorination is strongly related with the irreversible adsorption of chlorine species. To explain the cause of unique activity and stability of AgSiBEA additional HRTEM, STEM and EDS-elemental mapping investigations for spent samples were done (**Figs 10, 11** and **12**). **Figs. 10 and 11** show the typical STEM images and EDS-elemental mapping of Ag (blue), Cl (green), for spent-red-C-$Ag_{2.0}$HAlBEA and spent-red-C-$Ag_{2.0}$SiBEA. It was shown that very small silver nanoparticles present in both of the catalysts are resistant for chlorination. Ensures this phenomenon, very small silver nanoparticles show unique activity and stability in conversion of 1,2-dichloroethane towards value added product (ethylene**) Figs. 6,7,11.** Further

identification of phases (**Fig.12**) has confirmed phenomenon of the formation of AgCl from larger silver nanoparticles and chlorine resistance of < 3 nm Ag nanoparticles.

3.5. X-ray diffraction investigation

The similar X-ray diffractograms of red-C-$Ag_{2.0}$HAlBEA, red-C-$Ag_{2.0}$SiBEA, spent-red-C-$Ag_{2.0}$HAlBEA and spent-red-C-$Ag_{2.0}$SiBEA (**Fig. 13**) indicate that the calcination, acid treatment as well as reaction condition did not affect crystallinity of zeolite materials.

The introduction of silver into HAlBEA zeolite led to little shift of main, narrow diffraction peak from $2\theta = 22.44^{o}$ (for HAlBEA) [21] to $2\theta = 22.52^{o}$ (for red-C-$Ag_{2.0}$HAlBEA) (**Fig. 13**). It indicates that introduction of silver ions in the HAlBEA support and the further calcination and reduction of as prepared $Ag_{2.0}$HAlBEA zeolite do not result in significant changes of BEA structure. In addition, XRD of spent-red-C-$Ag_{2.0}$HAlBEA did not show any changes in the position of the main diffraction peak. It indicates the stability of BEA zeolite structure under reaction condition and not as strong interaction of chlorine containing species with acidic active sites as it was observed earlier [21].

Different situation was observed in case of silver catalyst prepared by two-step postsynthesis method. Incorporation of Ag ions into dealuminated form of BEA led to significant shift of the main diffraction peak from $2\theta = 22.70^{o}$ (for SiBEA) [21] to $2\theta = 22.48^{o}$ (for red-C-$Ag_{2.0}$SiBEA) (**Fig. 13**). This phenomenon suggests that the incorporation of Ag^{+} ions into vacant-T-atom sites of SiBEA support and the further calcination and reduction of as resulted $Ag_{2.0}$SiBEA zeolite led to significant expansion of BEA matrix. For spent-red-C-$Ag_{2.0}$SiBEA the position of the main diffraction peak changed only a little to $2\theta = 22.52^{o}$ indicated some interaction of chlorine containing species with silver active centres during HDC of 1,2-DCE.

Moreover, comparative study between XRD results obtained for red-C-$Ag_{2.0}$HAlBEA, red-C-$Ag_{2.0}$SiBEA, spent-red-C-$Ag_{2.0}$HAlBEA and spent-red-C-$Ag_{2.0}$SiBEA have shown that AgCl is formed under reaction condition on both catalysts (**Fig. 13**). However, this phenomenon does not affect catalytic activity of red-C-$Ag_{2.0}$SiBEA (**Figs. 4,7**) that shows the same conversion of 1,2-dichloroethane during more than 66 h of reaction time. These results are in line with the results obtained by transmission electron microscopy (**Figs 8-12**), and confirmed the transformation of larger silver nanoparticles into AgCl (**Figs 9-12**). Thereby, they confirmed the beneficial role of very small nanoparticles of silver, resistant to deactivation in hydrodechlorination of 1,2-dichloroethane.

Conclusions

The investigations carried out in this work have revealed the unique activity of monometallic silver containing zeolite catalysts in the conversion of 1,2-dichloroethane into value added products. The role of silver in red-C-$Ag_{2.0}$SiBEA and red-C-$Ag_{2.0}$HAlBEA was different.

We have showed, that the excellent activity of silver catalyst prepared by two-step postsynthesis method in the conversion of 1,2-DCE (with 100% selectivity to ethylene) is strongly related to the presence of very small (< 3 nm) silver nanoparticles in red-C-$Ag_{2.0}$SiBEA, resistant to deactivation.

On the other hand, the activity of red-C-HAlBEA support and red-C-$Ag_{2.0}$HAlBEA material is related to the presence in both catalysts strong Brønsted acidic centres that played key role in conversion of 1,2-dichloroethane to vinyl chloride (100 % selectivity).

Acknowledgements

Project funded by the Foundation for Polish Science, POMOST/2011-4/11 co-financed by the EU European Regional Development Fund (AŚ, SD). Special thanks for Ilona Zielińska for participation in the catalytic experiments.

References

1. B. Huang, Ch. Lei, Ch. Wei, G. Zeng, Environ Int 71 (2014) 118-138
2. L.E. Manzer, V.N. Rao, Adv. Catal. 39 (1993) 329-350
3. M. Wu et al. Catal. Commun. 18 (2012) 72–75
4. R. López-Fonseca, J. I. Gutiérrez-Ortiz, J. L. Ayastui, M.A. Gutiérrez-Ortiz, J. R. González-Velasco, Appl. Catal. B 45 (2003) 13–21
5. S. Pitkäaho, T. Nevanperä, L. Matejova, S. Ojala, R. L. Keiski, Appl. Catal. B: 138–139 (2013) 33–42
6. Y-F Wang, W-J. Lee, Ch-Y Chen., J. Aerosol Sci. 28, Suppl. 1, (1997)
7. P.H. Taylor, B. Dellinger, J. Anal. Appl. Pyrolysis 49 (1999) 9–29
8. J. Kawabata, I.A. Take, Y. Ohishi, T. Shishido, Y. Tiaw, K. Takachi, K. Takeshira, Appl. Catal. B 66: (2006) 151-160
9. Y. Cesteros, P. Salagre, F. Medina, J.E. Sueiras, Catal Lett. 79 (2002) 83-88
10. N. Martín, A. López-Gaona, M. Viniegra, P. Villamil, G. Córdoba, Reac. Kinet. Mech. Catal. 101 (2010) 491–500
11. N. Barrabès, K. Fottinger, J. Llorca, A. Dafinov, F. Medina, J. Sa, C. Hardacre, G. Rupprechter, J. Phys. Chem. C 114 (2010) 17675–17682
12. B.T Meshesha, N. Barrabes, J. Llorcac, A. Dafinov, F. Medina, K. Fottinger, Appl. Catal. B 117– 118 (2012) 236– 245
13. A. Śrebowata, W. Lisowski, J.W. Sobczak, Z. Karpiński, Catal. Today 175 (2011) 576–584

14. B.T. Meshesha , N. Barrabes, K. Fottinger, R.J. Chimentao, J. Llorca, F. Medina, G. Rupprechter, J.E. Sueiras, Appl. Catal. A 453 (2013) 130–141
15. X. Wei, A. Wang, X. Yang, L. Li, T. Zhang, Appl. Catal. B 121–122 (2012) 105–114
16. Y. Han, J. Zhou, W. Wang, H. Wan, Z. Xu, Sh. Zheng, D. Zhu, Appl. Catal. B 125 (2012) 172–179
17. P P. Kulkarni, V. I. Kovalchuk, J. L. d'Itri, Appl. Catal. B 36 (2002) 299–309
18. S. Lambert, F. Ferauche, A. Brasseur, J.-P. Pirard, B. Heinrichs, Catal. Today 100 (2005) 283–289
19. K.V.R. Chary, P.V.R. Rao, V.V. Rao, Catal. Commun. 9 (2008) 886–893
20. A. Śrębowata, W. Juszczyk, Z. Kaszkur, J.W. Sobczak, L. Kępiński, Z. Karpiński, Appl. Catal. A 319 (2007) 181–192
21. A. Śrębowata, R. Baran, D. Łomot,D. Lisovytskiy, T. Onfroy, S. Dzwigaj, Appl. Catal. B 147 (2014) 208-220
22. S. Lambert, A. Brasseur, J.P. Pirard, B. Heinrichs, Appl. Catal. A 270 (2004) 201–208.
23. A. Śrębowata, R. Baran, S. Casale, I. I. Kamińska, D. Łomot, D. Lisovytskiy, S. Dzwigaj, Appl. Catal. B 152–153 (2014) 317-327
24. A. Śrębowata, W. Juszczyk, Z. Kaszkur, Z. Karpiński, Catal. Today124 (2007) 28-35
25. H. Lee, S.J. Schmieg, S.H. Oh, Appl. Catal. A 342 (2008) 78–86
26. N. Popovych, P. Kyriienko, S. Soloviev, S. Orlyk, S. Dzwigaj, Micropor. Mesopor. Mater. 203 (2015) 163-169
27. L. Gang, B.G. Anderson, J. van Grondelle, R.A. van Santen, Appl. Catal. B 40 (2003) 101-110
28. E. Kolobova, A. Pestryakov, A. Shemeryankina, Y. Kotolevich, O. Martynyuk, H.J. Tiznado Vazquez, N. Bogdanchikova, Fuel 138 (2014) 65-71
29. T. C.R. Rocha, M. Hävecker, A. Knop-Gericke, R. Schlögl, J. Catal. 312 (2014), 12-16

30. P. Claus, H. Hofmeister, J. Phys.Chem. B 103 (1999) 2766–2775

31. H. Zea, K.Lester ,A.K. Datye, E. Rightor, R. Gulotty, W. Waterman ,M. Smith, Appl. Catal. A 282 (2005) 237–245

32. N. Job, B. Heinrichs, F. Ferauche, F. Noville, J. Marien, J-P Pirard, Catal. Today 102–103 (2005) 234–241

33. A. Śrębowata, I. Zielińska, R. Baran, G. Słowik, S. Dzwigaj. Catal.Commun. 69 (2015) 154–160

34. R. Seifert, R. Rytz, G. Calzaferri, J. Phys. Chem. A 104 (2000) 7473-7483

35. G. Calzaferri, C. Leiggener, S. Glaus, D. Schürch, K. Kuge, Chem. Soc. Rev. 32 (2003) 29-37

36. J. Shibata, K. Shimizu, Y. Takada, A. Shichi, H. Yoshida, S. Satokawa, A. Satsuma, T. Hattori, J. Catal. 227 (2004) 367-374

37. A. Satsuma, J. Shibata, A. Wada, Y. Shinozaki, T. Hattori, Stud. Surf. Sci. Catal. 145 (2003) 235-238

38. Ch. Hu, T. Peng, X. Hu, Y. Nie, X. Zhou, J. Qu, H. He J. Am. Chem. Soc. 2010, 132, 857–862

39. K. Sato, T. Yoshinari, K. Kintaichi, M. Haneda, H. Hamada, Appl. Catal. B. 44 (2003) 67-78

40. M. Matsuoka, E.Matsuda, K. Tsuji, H. Yamashita, M. Anpo, J. Mol. Catal. A 107 (1996) 399–403

41. J. Texter, T. Gonsiorowski, R. Kellerman, Phys. Rev. B. 23 (1981) 4407–4418

42. S. Dzwigaj, N. Popovych, P. Kyriienko, J.-M. Krafft, S. Soloviev, Micropor. Mesopor. Mater. 182 (2013) 16-24

43. K. Fuku, R. Hayashi, S. Takakura, T. Kamegawa, K. Mori, H. Yamashita, Angew. Chem. Int. Ed. 2013, 52, 7446 –7450

44. D. Chen, Z. Qu, S. Shen, X. Li, Y. Shi, Y. Wang, Q. Fu, J. Wu, Catal. Today 175 (2011) 338–345

45. S.G. Aspromonte, E.E. Miró, A.V. Boix, Adsorption 18 (2012) 1–12

46. S.C. Shekhar, J.K. Murthy, P.K. Rao, K.S.R. Rao, Appl. Catal. A: Gen. 271 (2004) 527; 95–101

47. E.V. Golubina, E.S. Lokteva, V.V. Lunin, N.S. Telegina, A.Yu. Stakheev, P. Tundo, Appl. Catal. A: Gen. 302 (2006) 32–41

48. V.I. Simagina, O.V. Netskina, E.S.Tayban, O.V. Komova, E.D. Grayfer, A.V. Ischenko, E.M. Pazhetnov, Appl. Catal. A: Gen. 379 (2010) 87–94

49. S. L. Pirard, J-P. Pirard, G. Heyen, J-P. Schoebrechts, B. Heinrichs, Chem. Eng. J. 173 (2011) 801– 812

50. N. S. Babu, N. Lingaiah, Nayeem Pasha, J. Vinod Kumar, P.S. Sai Prasad, Catal. Today, 141 (2009) 120-124

51. M. Bonarowska, Z. Kaszkur, L. Kępiński, Z. Karpiński Appl. Catal. B 99 (2010) 248-256

52. S. Gómez-Quero, F. Cárdenas-Lizana , M. A. Keane, J. Catal. 303 (2013) 41– 49.

Figure captions

Figure 1. DR UV-vis spectra recorded at ambient atmosphere of as prepared ($Ag_{2.0}$HAlBEA), calcined (C-$Ag_{2.0}$HAlBEA) and further reduced (red-C-$Ag_{2.0}$HAlBEA) Ag-containing HAlBEA.

Figure 2. DR UV-vis spectra recorded at ambient atmosphere of as prepared ($Ag_{2.0}$SiBEA), calcined (C-$Ag_{2.0}$SiBEA) and further reduced (red-C-$Ag_{2.0}$SiBEA) Ag-containing SiBEA.

Figure 3. Temperature programmed reduction profiles of C-$Ag_{2.0}$HAlBEA and C-$Ag_{2.0}$SiBEA.

Figure 4. Time on stream behavior of red-C-HAlBEA, red-C-$Ag_{2.0}$HAlBEA, red-C-SiBEA, and red-C-$Ag_{2.0}$SiBEA catalysts in hydrodechlorination of 1,2-dichloroethane at 523 K: overall conversion.

Figure 5. Time on stream behavior of red-C-HAlBEA, red-C-$Ag_{2.0}$HAlBEA, red-C-SiBEA, and red-C-$Ag_{2.0}$SiBEA catalysts in hydrodechlorination of 1,2-dichloroethane at 523 K: vinyl chloride selectivity.

Figure 6. Time on stream behavior of red-C-HAlBEA, red-C-$Ag_{2.0}$HAlBEA, red-C-SiBEA, and red-C-$Ag_{2.0}$SiBEA catalysts in hydrodechlorination of 1,2-dichloroethane at 523 K: ethylene selectivity.

Figure 7. Time on stream behavior of red-C-$Ag_{2.0}$SiBEA catalyst in long term hydrodechlorination of 1,2-dichloroethane at 523 K: ethylene selectivity and overall conversion.

Figure 8. HRTEM images and silver nanoparticle size distribution of red-C-$Ag_{2.0}$HAlBEA and spent-red-C-$Ag_{2.0}$HAlBEA .

Figure 9. HRTEM images and silver nanoparticle size distribution of red-C-$Ag_{2.0}$SiBEA and spent-red-C-$Ag_{2.0}$SiBEA.

Figure 10. STEM images with EDS elemental mapping for spent-red-C-$Ag_{2.0}$HAlBEA.

Figure 11. STEM images with EDS elemental mapping for spent-red-C-$Ag_{2.0}$SiBEA.

Figure 12. HRTEM images with identification of Ag and AgCl phases for spent-red-C-$Ag_{2.0}$HAlBEA and spent-red-C-$Ag_{2.0}$SiBEA.

Figure 13. XRD patterns of red-C-$Ag_{2.0}$HAlBEA, spent-red-C-$Ag_{2.0}$HAlBEA, red-C-$Ag_{2.0}$SiBEA and spent-red-C-$Ag_{2.0}$SiBEA. Circles indicate positions of XRD reflections of Ag (111), triangles symbolize positions of XRD reflections of AgCl (002).

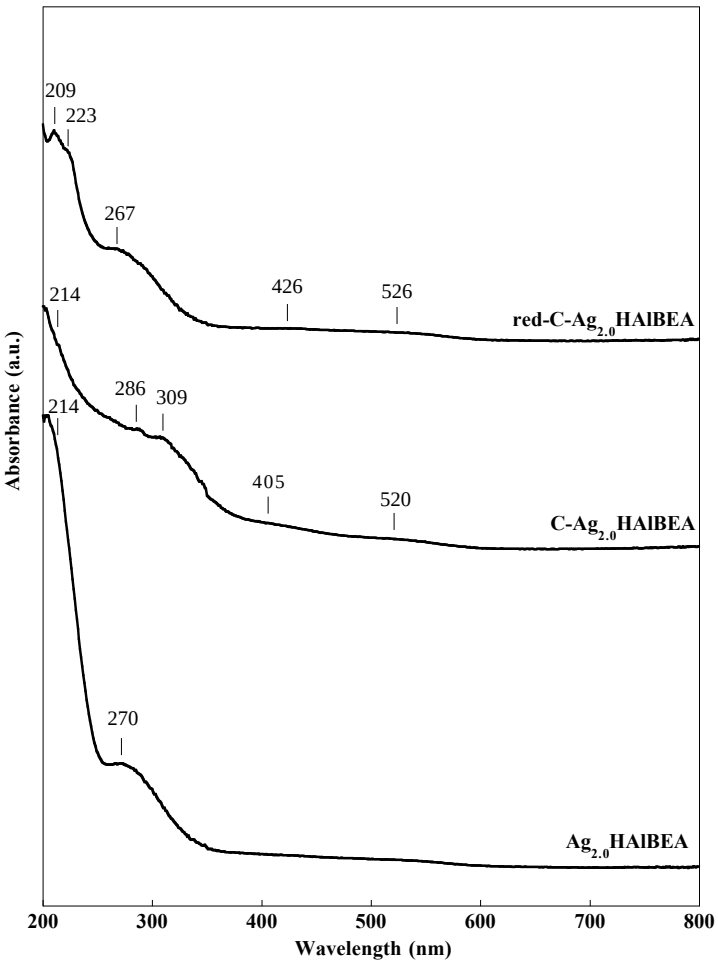

Figure 1

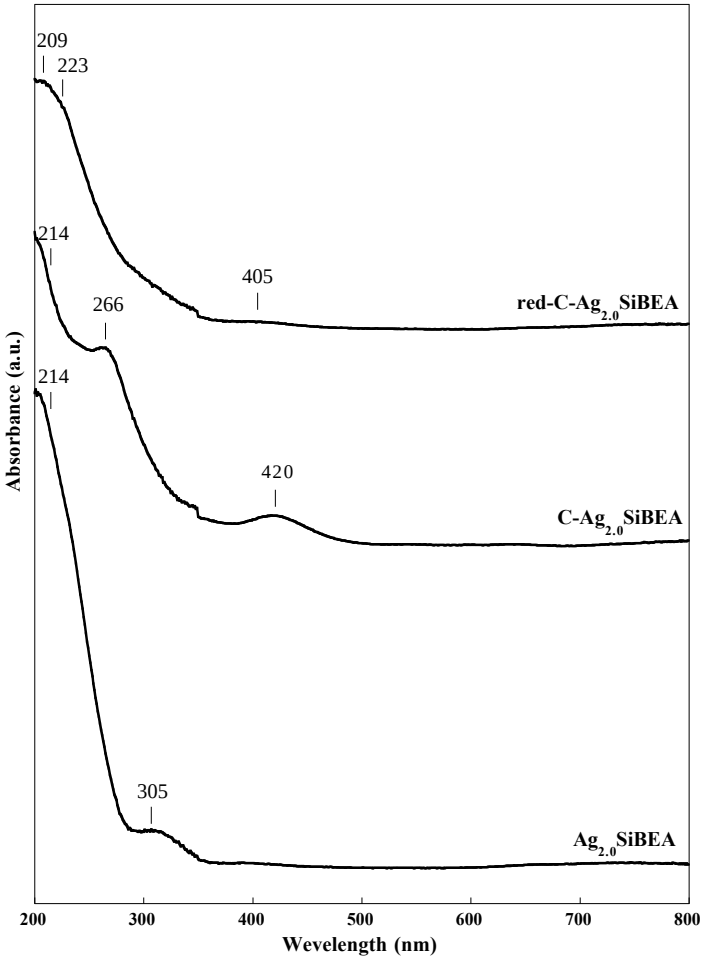

Figure 2

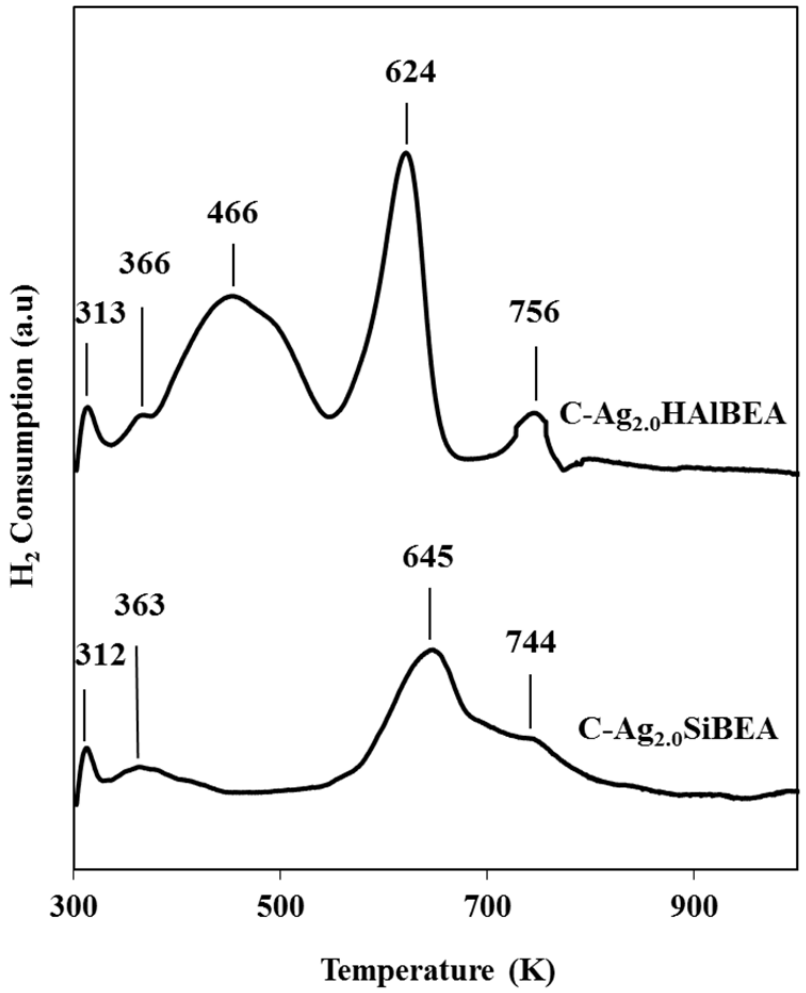

Figure 3

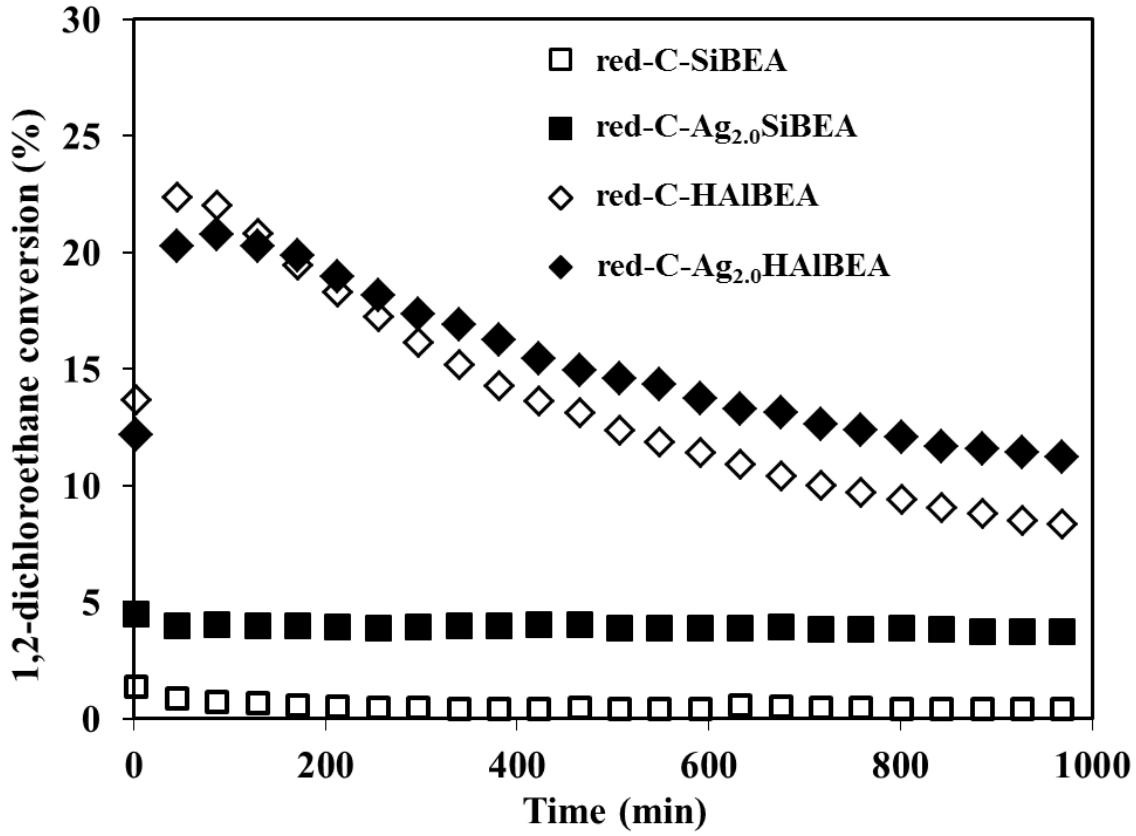

Figure 4

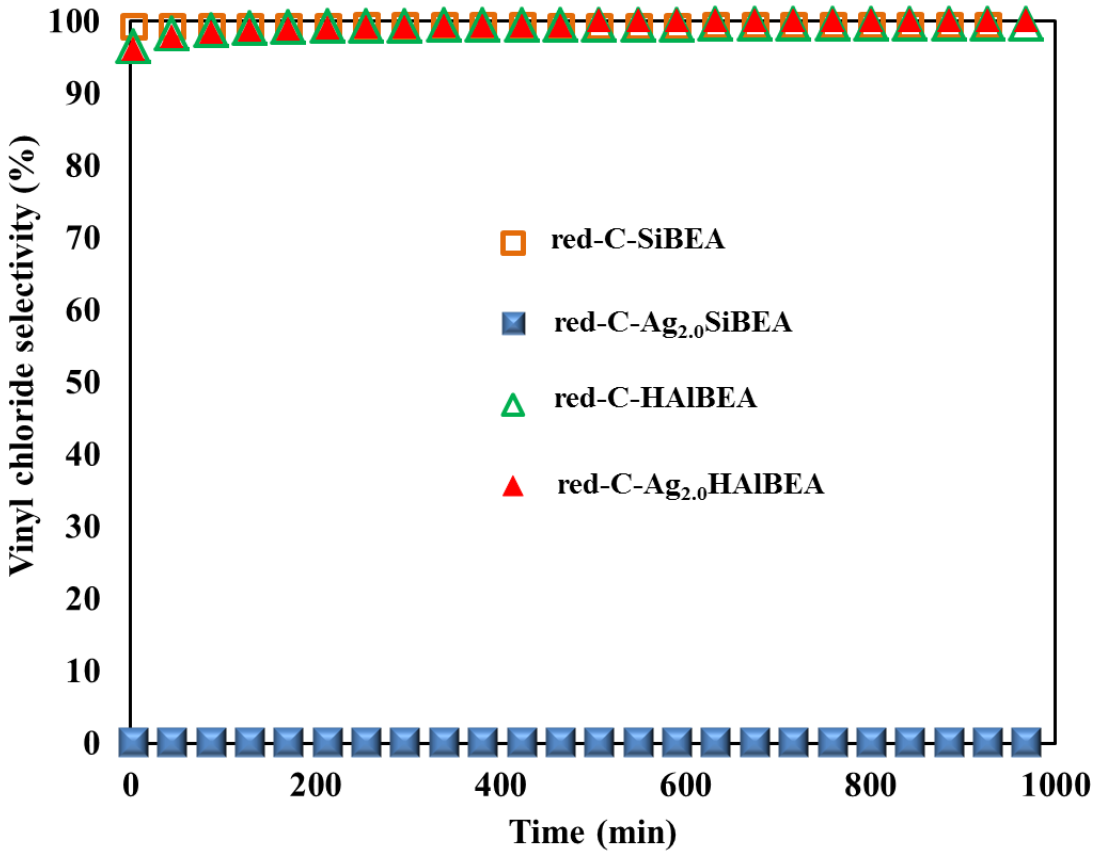

Figure 5

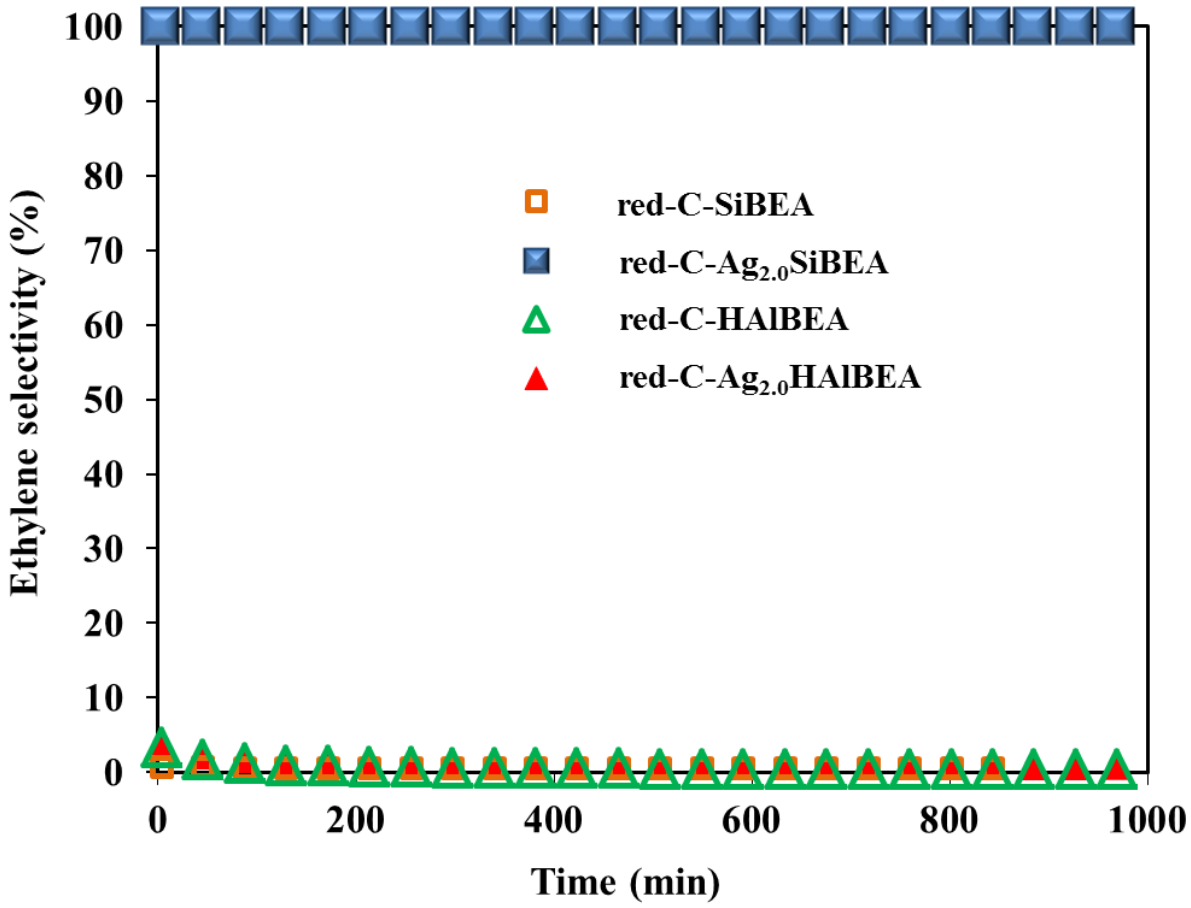

Figure 6

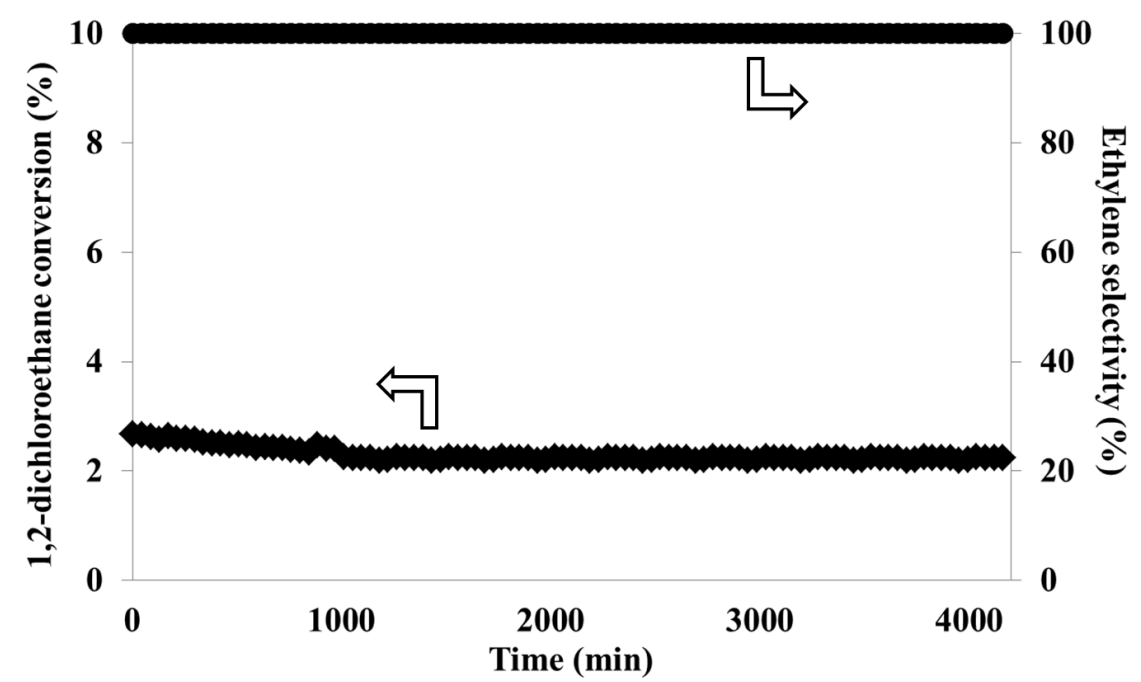

Figure 7

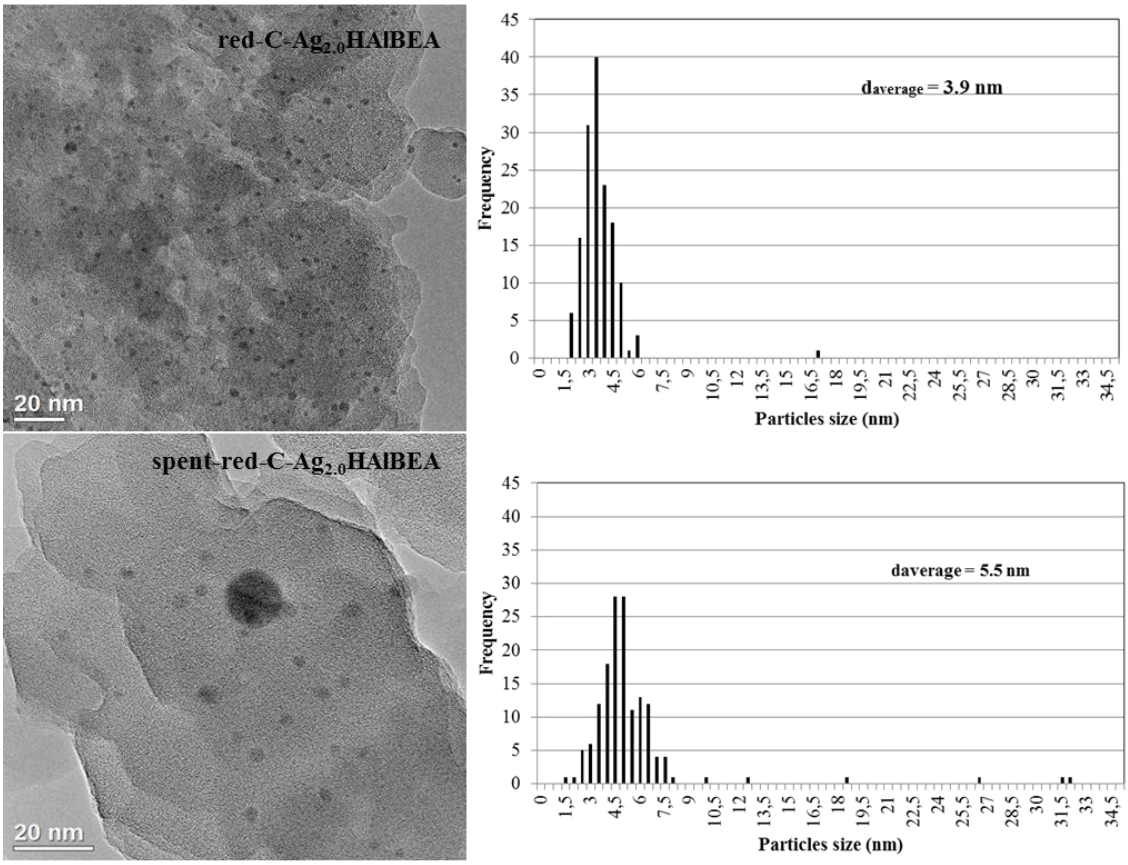

Figure 8

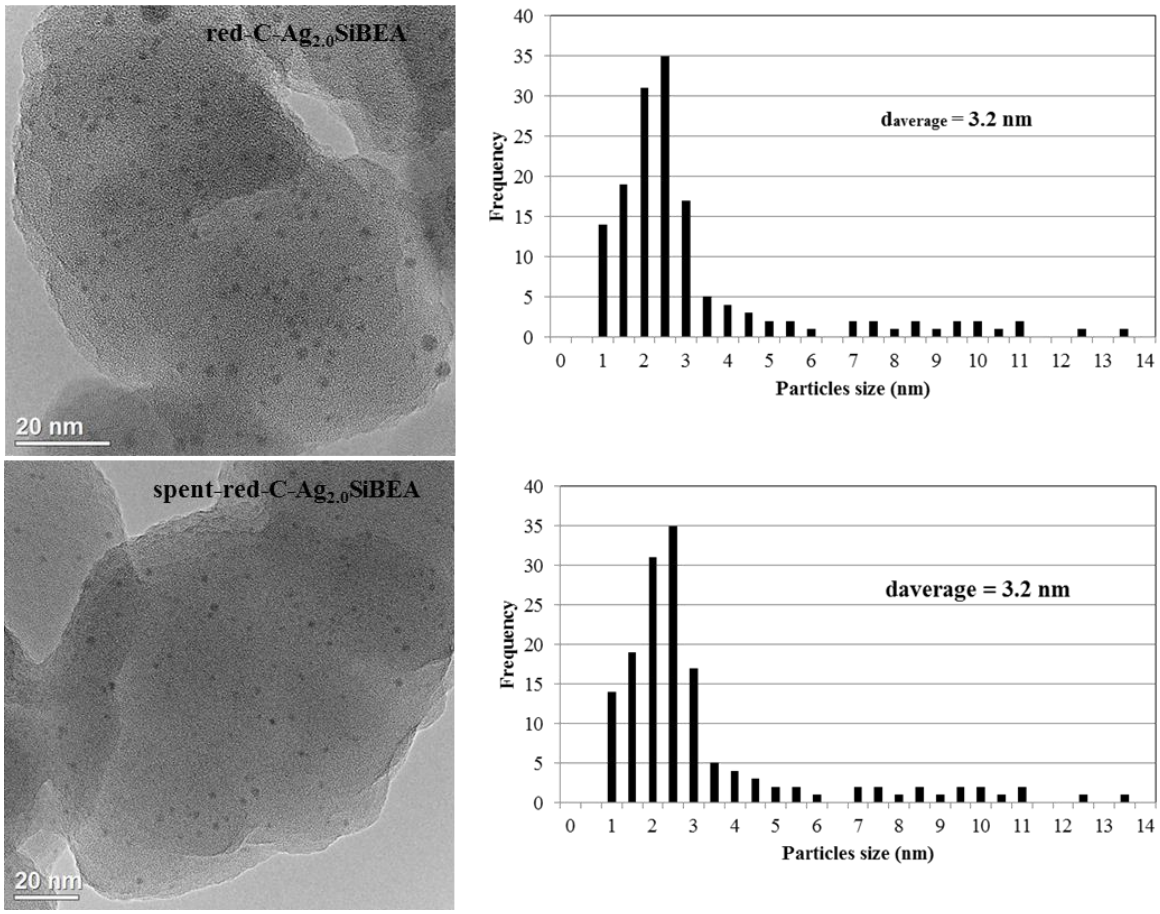

Figure 9

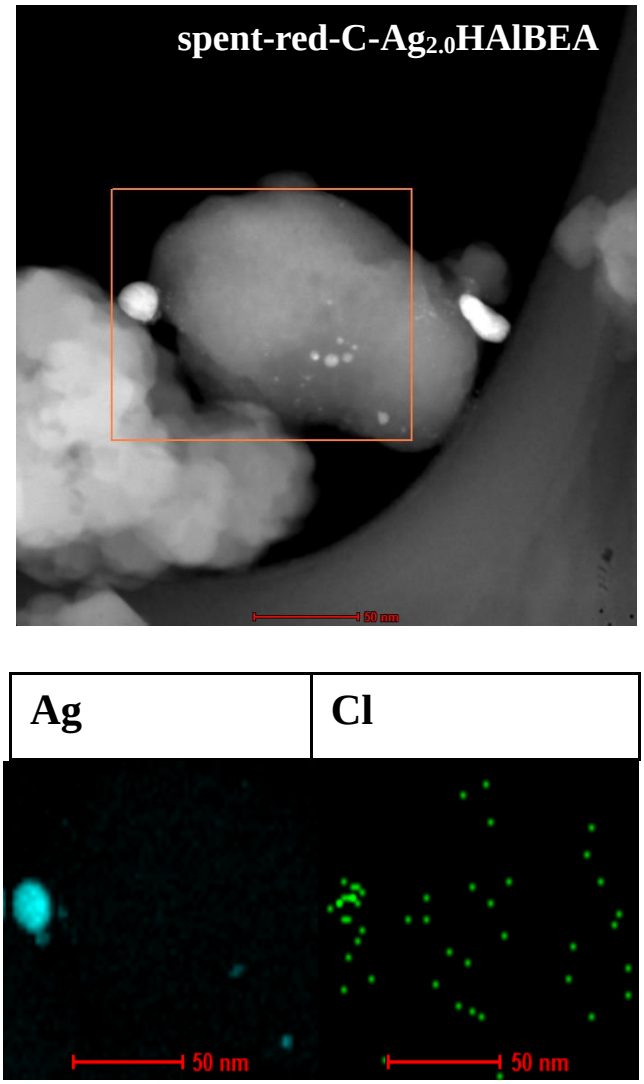

Figure 10

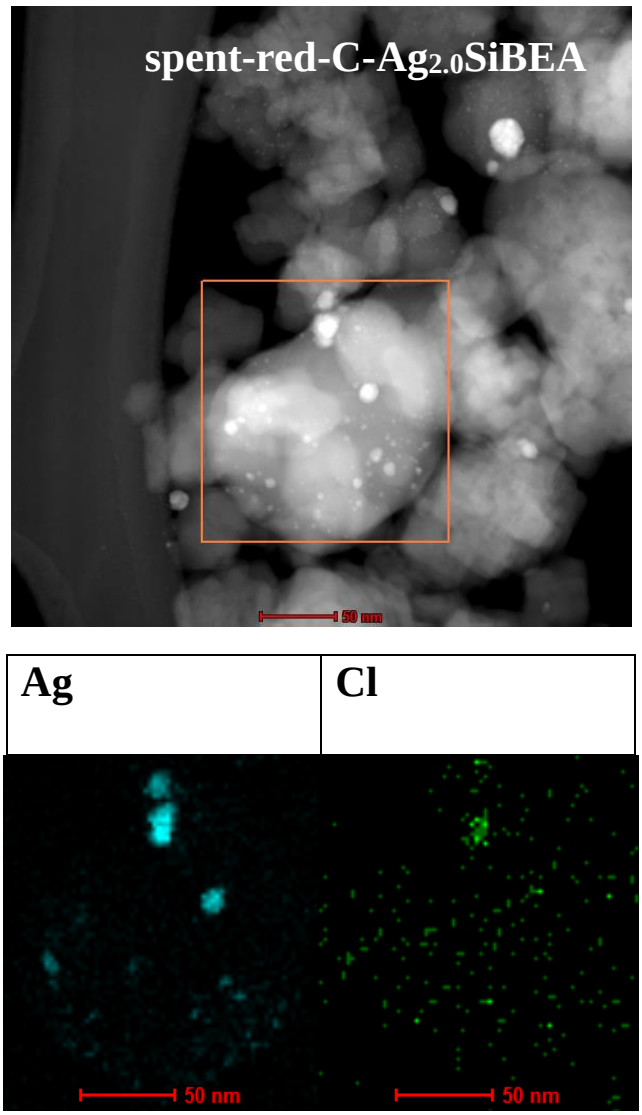

Figure 11

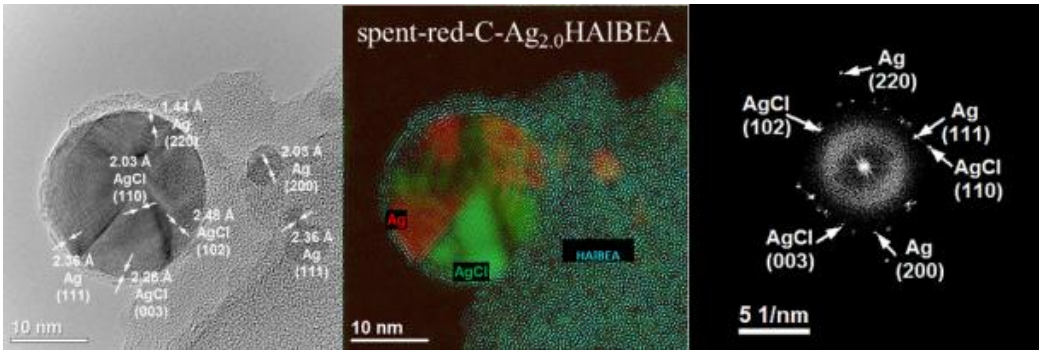

Figure 12

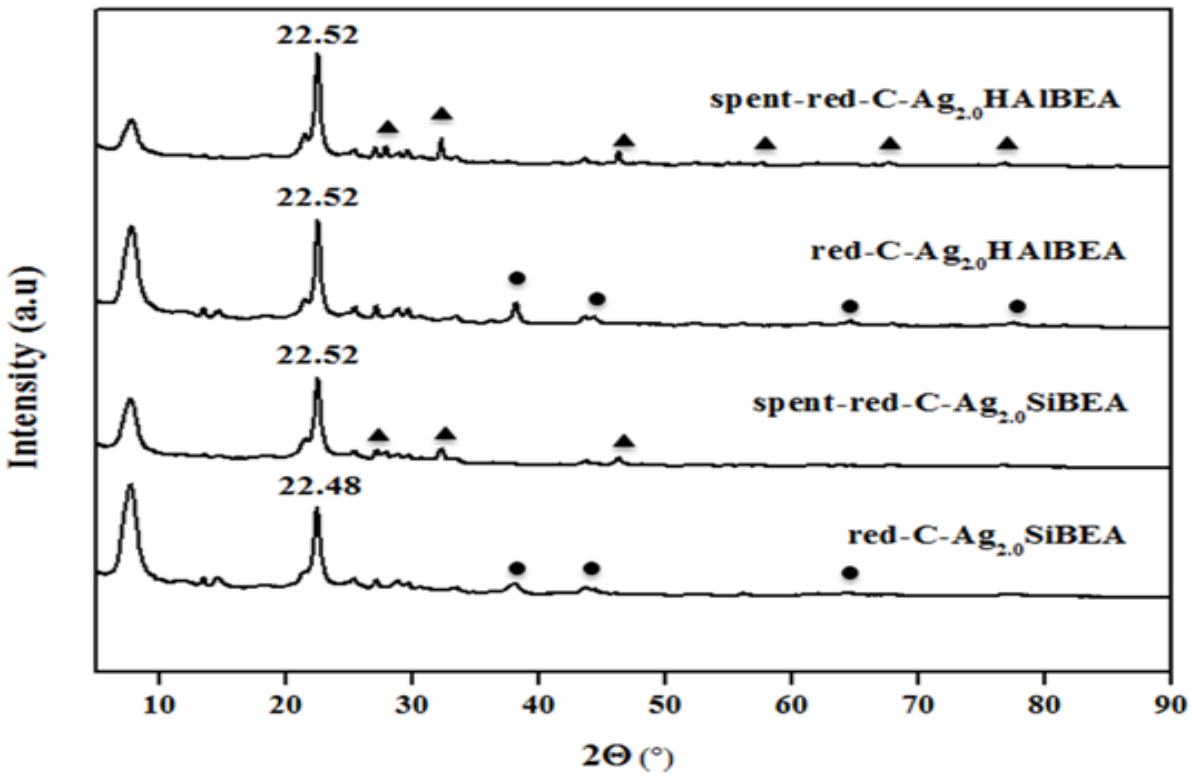

Figure 13